

Manifestation of quantum chaos on scattering techniques: application to low-energy and photo-electron diffraction intensities.

P.L. de Andres and J.A. Vergés

Instituto de Ciencia de Materiales, Consejo Superior de Investigaciones Científicas, Cantoblanco, E-28049 Madrid, Spain
(June 28, 2017)

Intensities of LEED and PED are analyzed from a statistical point of view. The probability distribution is compared with a Porter-Thomas law, characteristic of a chaotic quantum system. The agreement obtained is understood in terms of analogies between simple models and Berry's conjecture for a typical wavefunction of a chaotic system. The consequences of this behaviour on surface structural analysis are qualitatively discussed by looking at the behaviour of standard correlation factors.

PACS numbers: 61.14.Dc, 61.14.Hg, 05.45.+b

There is a continuous interest in understanding the relationship between chaos and quantum mechanics. Long time ago, Wigner investigated the influence of chaos on quantum mechanical scattering experiments in nuclear systems.¹ Thereafter, much work has concentrated on the analysis of energy levels of bound states inside closed systems (like various types of billiard geometries). While these studies offer obvious advantages, a great deal of information is lost by neglecting the examination of the wavefunctions. In fact, a good understanding of wavefunctions is crucial to explain open systems, like the standard probe-target-detector setup used in most scattering experiments. Therefore, it is quite perplexing to find so few examples in the literature related to quantum chaos manifested in experiments where wavefunctions are analyzed, which should be emphasized, only correspond to closed geometries.^{2,3} In this work, we show that reflected intensities of surface scattering experiments, which are directly related to the modulus squared of the wavefunction, are consistent with quantum chaos. Therefore, we are proposing a new class of simple experimental systems where quantum chaos is manifested in the properties of wavefunctions.

One reason to expect quantum chaotic behaviour in a scattering experiment comes from the existence of classical chaos when three or more scattering potentials are involved.⁴ Actually, Mucciolo et al.⁵ have recently shown that the high energy region of the calculated band structure of Si and $\text{Al}_x\text{Ga}_{1-x}\text{As}$ is complex enough to obey the statistical distribution of levels corresponding to random matrix theory (RMT).⁶ Based on this statistical analysis, the authors claim that these systems exhibit quantum chaos. Although just a theoretical prediction, this is a remarkable result because no disorder or incommensurate geometries are involved, and the physical reason for chaos should be found elsewhere (e.g., the intrinsic multiple scattering (MS) originating Bloch states and giving rise to the crystal band structure).

In this letter, the manifestation of chaos on standard surface scattering techniques like Low Energy Electron Diffraction (LEED) or Photoelectron Diffraction (PED) is investigated. These techniques are dominated in most experimental systems by MS, yielding a clear similitude to the band structure problem mentioned above. In surface structural work, it is a common belief that MS intro-

duces a richer but more difficult analysis. This general statement is analyzed here from the point of view of the chaotic component of the LEED and PED experiments, while we draw new attention to a class of quantum systems obeying a Porter-Thomas probability distribution.⁷ Ultimately, our aim is the understanding of the relationship between complex scattering phenomena and the emergence of quantum chaos.

To characterize chaotic wavefunctions Porter and Thomas⁷ advanced the hypothesis that wavefunctions of a chaotic system should display a χ_ν^2 statistical probability distribution. Subsequently, this hypothesis has been rigorously justified using the supersymmetry formalism,⁸ and has been used as a convenient definition of quantum chaos, that at least can be thought as a necessary condition. Dyson⁹ demonstrated that within the RMT only three universal classes can exist depending on whether the hamiltonian is constructed with real numbers, complex numbers or quaternions, corresponding respectively to $\nu = 1, 2$, and 4 degrees of freedom. Since scattering wavefunctions are complex numbers, the statistics corresponding to the universality class $\nu = 2$ is expected.

An interesting theoretical result on the wavefunction of a chaotic system is due to Berry.¹⁰ Analysing the semiclassical mechanics of regular and irregular motion, he realized that a typical chaotic wavefunction should be a linear combination of plane waves with random \vec{k} -orientations, (at a fixed constant energy), and random complex coefficients:

$$\psi_{\vec{k}}(\vec{x}) \propto \sum_{j=1, N} a_j e^{i\delta_j} e^{i\vec{k}_j \cdot \vec{x}} \quad (1)$$

Heller et al.¹⁰ have further investigated the properties of these chaotic wavefunctions, finding that in 2D they present characteristic scars. Berry's chaotic wavefunction can be interpreted as the result of multiple random reflections of a plane wave. It can also be thought as the superposition of plane waves originating at N points propagating with the same energy in random orientations, and mixed with appropriated coefficients. Guided by these images, we try to find a physical system where a similar wavefunction can be realized.

First of all, we consider a PED experiment where an electron inside an atomic core is excited by an incident X-

ray photon, to be subsequently diffracted by a cluster of n atoms surrounding the original source. This is a complicated scenario, but making some approximations that have been tested in the literature, a simple expression for the wavefield at a distance R (far-field) is:¹¹

$$\psi_k(\hat{k}) = \frac{e^{ikR}}{ikR} \left(1 + \sum_{\omega=1}^{n+\binom{n}{2}+\dots} c_{\vec{r}_\omega} e^{-i\vec{k}\vec{r}_\omega} \right), \quad (2)$$

where the complex coefficients, $c_{\vec{r}_\omega}$, include appropriated scattering factors and the expansion can be extended to any desired order of scattering. It is important to realize the similarity of this MS series with Berry's one: taking away the prefactor and the source wave, and given a fixed direction in real space determined by \hat{k} , it is written as a sum of N plane waves $e^{i\vec{k}\cdot\vec{r}_\omega}$ with complex coefficients, where the many \vec{r}_ω may result oriented in uncorrelated directions if enough scattering is allowed. The following question arises in this context: how many plane waves are necessary to allow Eq. (1) to follow a Porter-Thomas statistical distribution? As an example, if $k = 2\pi$, we find that just $N = 10$ are enough to find a reasonable agreement (e.g., see Fig. 1); the result for as few as $N = 2$ is given in the same figure for comparison.

Secondly, we notice that an expression that is formally similar to Eq. (2) can be written for the Diffuse LEED (DLEED) wavefield:¹²

$$\psi_k(\hat{k}) = F_0(\vec{k})e^{i\vec{k}\cdot\vec{r}} + \sum_{\alpha} F_{\alpha}(\vec{k})e^{i\vec{k}\cdot(\vec{r}-\vec{r}_{\alpha})}, \quad (3)$$

where F_{α} represent generalized scattering factors including MS contributions. Standard LEED I(V) curves can be described in the same way, for a given energy, just keeping in mind that if the system exhibits perfect periodicity in the parallel direction, only a discrete set of points given by Bragg conditions are available.

Before trying to analyze real experiments, a set of controlled theoretical simulations of relevant systems is considered. We investigate the behaviour of the single scattering term in Eq. (2) performing the summation over a set of 500 atoms randomly distributed around the origin between $r_{\alpha} = 10$ a.u. and $r_{\alpha} = 150$ a.u. (atomic units will be used throughout the paper, expressing distances in Bohrs and energies in Hartrees). The central region (magnified ten times) of a typical $|\psi_k|^2$ ($k = 6$ a.u.) measured on a sphere at an asymptotic distance is shown in Fig. (2). A typical *worm-like* image is obtained when the pattern saturates at high energies or high r_{α} distances. The corresponding probability distribution of intensities (normalized to the average) is seen to follow a χ_2^2 distribution rather well.

Using the same model, we explore the probability distribution of intensities produced by a small quasi-regular cluster of atoms. A cube of $2 \times 2 \times 2$ Ni atoms centered around the origin at a distance of 5 a.u is chosen. Phase shifts up to $l_{max} = 7$ are used to compute the scattering

factors. These phase shifts have been obtained from a muffin-tin model, and can be used to represent the scattering of electrons by atoms in the real structure. In order to simulate small geometrical irregularities caused by relaxations, reconstructions or simply the effect of temperature, the atoms are randomly displaced from their perfect positions in the cube with values uniformly distributed between 0 and $\sqrt{3}d$. Fig. 1 shows the result of such a simulation for $d = 1$ a.u.. The agreement with the Porter-Thomas law is really good. In the same figure, the effect of a smaller arbitrary displacement ($d = 0.2$ a.u.) is also shown, together with a similar calculation for a double-scattering term in a cubic array of $3 \times 3 \times 3$ Ni atoms with comparable results. The analysis of Eq. (1) proves that fluctuations are responsible for the appearance of the ideal Porter-Thomas distribution. Therefore, the deviations from the χ_2^2 distribution observed for the scattering series should be explained by studying their fluctuations, which is beyond the scope of this work.

We compute full dynamical diffuse Leed intensities¹³ for a realistic adsorption geometry on the system O/Ni(100) (oxygen is placed on the hollow site at 1.51 a.u. from the surface). All parameters are taken from a detailed structural analysis of the same system.¹⁴ It is worthwhile to notice two points: i) All the Ni atoms are placed at ideal bulk-like positions. Therefore, there is not geometrical disorder in the problem, the main source of complexity being MS by the atoms in the ordered lattice; and, ii) All the calculations are performed at $T = 0$ K, although attenuation effects are taken into account in this formalism via an imaginary part ($V_{0i} = 0.15$ a.u.) added to the energy. Fig. 3 shows the probability distribution for intensities calculated theoretically at three different energies (12, 14 and 16 a.u.), yielding a similar agreement to the Porter-Thomas probability distribution as the previous PED example. The same results are expected from the analysis of experimental intensities. As an example, Fig. 3 includes a single energy (11.1 a.u.) extracted from the experimental database measured by the Erlangen group.¹⁵

The same Porter-Thomas probability distribution should also appear when conventional LEED I(V) curves are analyzed, because our arguments above are valid for *any* energy. We have simulated theoretically the LEED I(V) curves¹⁸ for three materials with very different structures: Cu(100), W(100), and Si(111). An arbitrary non-normal incidence angle ($\theta = 20^\circ$, $\phi = 30^\circ$) breaking the symmetry is chosen. This yields the maximum number of inequivalent beams increasing the statistical confidence of the analysis. The first 9 emergent beams are used for Cu and W while the first 13 were chosen for Si. The energy ranged from 50 to 450 eV for both metals and from 30 to 300 eV for the semiconductor, yielding a database of about 100 a.u., which is enough for our purposes and easily accessible to experiment. The imaginary part of the energy is fixed to a constant value of 0.15 a.u., and $T = 0$ K is used again. Finally, we analyze the experimental database for $c(8 \times 2)$ GaAs(100),¹⁶

formed by 13 different beams measured at normal incidence. Our results are shown in Fig. 4, displaying an agreement with the Porter-Thomas probability distribution similar to the other examples.

Guided by these results, we predict the existence of a region (II) in parameter space, P , where small changes in \vec{p} (each component defining a relevant parameter for the structure), result in rapid changes of the wavefunction. On intuitive grounds, it can be assumed that these changes must separate exponentially. This region is intermediate between two different ones: a perturbative region (I), as for sufficiently small changes in \vec{p} we expect perturbation theory to give a reasonable answer,¹⁷ and a random region (III) where wavefunctions for different structures are uncorrelated. The existence of these three regions is checked by analyzing two R-factors commonly used in surface structure analysis: (i) A root mean square displacement¹⁸ adapted for DLEED (R_2) and, (ii) the Pendry R-factor¹⁹ (R_P) often used with standard LEED.

We apply R_2 to compare theoretically calculated DLEED intensities for O/Ni(100) as a function of the adsorption height h . Arbitrarily, $h = 1.51$ a.u. is chosen as the reference. This is a clean and controlled theoretical experiment where only the position of one atom is changed, but to stay closer to reality, we also consider the behaviour of the R_P in a recent structural analysis of $c(2 \times 2)$ Si/Cu(110) I(V) curves, where the relaxation of the whole surface layer is considered.²⁰ Both cases show the existence of the three regions mentioned above. Region I is obviously well characterized by the existence of a minimum that imposes a quadratic dependence. Region III is also easily identified by the saturation of the R-factor: for R_P this happens by construction around 1 (the maximum value for R_P can be twice this value, but saturation starts at values greater than 0.6). For R_2 we observe that saturation occurs around the value obtained by comparing two sets of N random intensities, so the R-factor is normalized to this value. Region II may be characterized by plotting the $\ln(R)$ versus a relevant component of \vec{p} , and identifying the interval where it behaves like a straight line. When we use these ideas to analyze the data, we find that the quadratic region (I) extends approximately 0.04 Å for the DLEED case ($R_2 \leq 0.2$) and 0.05 Å for the conventional LEED analysis ($R_P \leq 0.25$). The exponential region (II) extends also 0.04 Å for DLEED ($R_2 \leq 0.5$), while it goes to 0.09 Å for the LEED experiment ($R_P \leq 0.6$). Finally, an uncorrelated region extends beyond these intervals, provided we do not approach a multiple coincidence minima. We notice that a perturbative technique where the perturbation in the potential is proportional to the atomic displacements (the so-called Tensor LEED first approximation¹⁷) is known to break down beyond ≈ 0.1 Å. This is close to regions I and II, considered respectively a truly perturbative region (quadratic) and the onset of the breakdown for the perturbative approach (exponential). These findings should bring more rigour to the standard R-factor analysis because our analysis allow to identify regions II

and III, where correlations must be taken as spurious, and offer a new theoretical explanation for the definitive failure of simple scattering methods in LEED.

We have analyzed typical wavefunctions for LEED and PED experiments in the light of Berry's proposal for a generic chaotic wavefunction. Our statistical analysis shows that scattering wavefunctions computed from several models (including perfectly ordered structures) follow the Porter-Thomas χ_2^2 distribution. This property is also obtained analyzing experimental data for LEED and DLEED. The physical origin of this behaviour is the complexity of the scattering. Attenuation effects taken into account via a complex optical potential fitted to experiments, and defects (relaxations or reconstructions) do not change this conclusion. Finally, analysing the behaviour of two different R-factors, we have argued the existence of three distinct regions, showing the rationale behind widely used rules about which R-factors are acceptable in standard structural work and which are not.

We are grateful to Prof. K. Heinz for making available to us his experimental DLEED data on O/Ni(100). This work has been supported by the CICYT under contracts num. PB94-053 and MAT94-0058.

-
- ¹ E.P. Wigner, e.g. see *Statistical Theories of Spectra: Fluctuations*, Ed. by C.E. Porter, Academic Press (New York, 1965).
 - ² H. Alt, H.-D. Gräf, H.L. Harney, R. Hofferbert, H. Lengeler, A. Richter, P. Schardt, V.A. Weidenmüller, *Phys. Rev. Lett.* **74**, 62 (1995).
 - ³ P.B. Wilkinson et al., *Nature* **380**, 608 (1996).
 - ⁴ M.C. Gutzwiller, *Chaos in Classical and Quantum Mechanics*, Springer Verlag (New York, 1990).
 - ⁵ E.R. Mucciolo, R.B. Capaz, B.L. Altshuler, J.D. Joannopoulos, *Phys. Rev. B* **50**, 8245 (1994).
 - ⁶ M.L. Mehta, *Random Matrices*, 2nd ed. (Academic Press, San Diego, CA, 1991).
 - ⁷ C.E. Porter, R.G. Thomas, *Phys. Rev.* **104**, 483 (1956).
 - ⁸ K.B. Efetov, V.N. Prigodin, *Phys. Rev. Lett.* **70**, 1315 (1993).
 - ⁹ F.J. Dyson, *J. Math. Phys.* **3**, 140 (1962).
 - ¹⁰ M.V. Berry, in *Chaotic Behaviour of Deterministic Systems*, Ed. by G. Looss, R. Helleman and R. Stora (North Holland, NY 1983), p. 171; P.O'Connor, J. Gehlen, E.J. Heller, *Phys. Rev. Lett.* **58**, 1296 (1987).
 - ¹¹ P.A. Lee and J.B. Pendry, *Phys. Rev. B* **11**, 2795 (1975); J.J. Barton and D.A. Shirley, *Phys. Rev. B* **32**, 1906 (1985)
 - ¹² D.K. Saldin and P.L. de Andres, *Phys. Rev. Lett.* **64**, 1270 (1990).
 - ¹³ J.B. Pendry and D.K. Saldin, *Surf. Sci.* **145**, 33 (1984); D.K. Saldin and J.B. Pendry, *Comput. Phys. Commun.* **42**, 399 (1986).
 - ¹⁴ U. Starke, P.L. de Andres, D.K. Saldin, K. Heinz and J.B. Pendry, *Phys. Rev. B*, **38**, 12277 (1988).

- ¹⁵ K. Heinz, private communication.
¹⁶ F.J. Palomares, Ph.D. thesis, Chap. 3 (pg. 66), Universidad Autonoma de Madrid, Madrid (1993).
¹⁷ P.J. Rous, J.B. Pendry, D.K. Saldin, K. Heinz, K. Müller, N. Bickel, Phys. Rev. Lett. **57** 2951 (1986); P.J. Rous, Ph.D. thesis, Chap. 6 (pg. 167), Imperial College of Science, Technology and Medicine, London (1986).
¹⁸ M.A. Van Hove and S.Y. Tong, *Surface Crystallography by LEED*, (Springer-Verlag, Berlin, 1979); M.A. Van Hove, W.H. Weinberg and C.M. Chan, *Low-Energy Electron Diffraction*, (Springer-Verlag, Berlin, 1986).
¹⁹ J.B. Pendry, J. Phys. C: Solid State Phys. **13** (1980) 937.
²⁰ C. Polop, et al., unpublished.

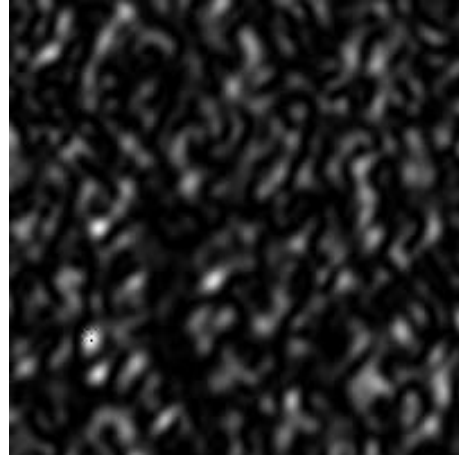


FIG. 2. Small portion of a wavefunction (modulus squared) obtained using Eq. (2) for a set of 500 atoms at random positions.

Figure 1

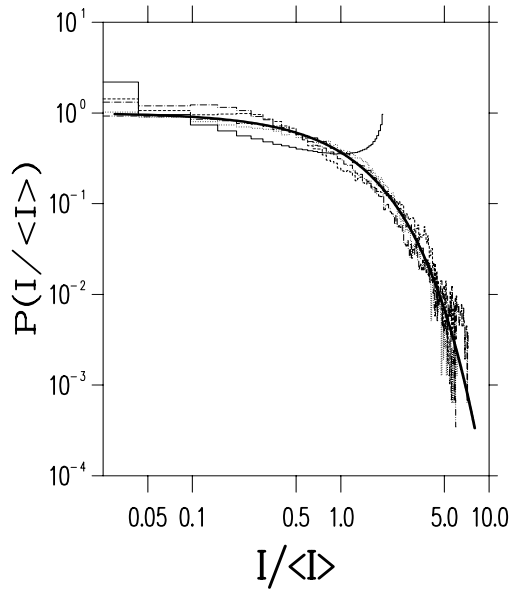


FIG. 1. Probability distribution for simplified models: (a) Thick solid line: χ_2^2 law; (b) Thin solid line: Berry's wavefunction with $N = 2$; (c) dashed-dotted line: Berry's wavefunction with $N = 10$; (d) dotted line: simple PED model for eight Ni atoms on a cube, simple scattering ($E = 1.8$ a.u., $d = 1.0$ a.u.); (e) dashed line: same as (d) with $d = 0.2$ a.u.; (f) dashed two-dotted line: simple PED model for 27 Ni atoms, double scattering ($E = 1.8$ a.u., $d = 1.0$ a.u.).

Figure 3

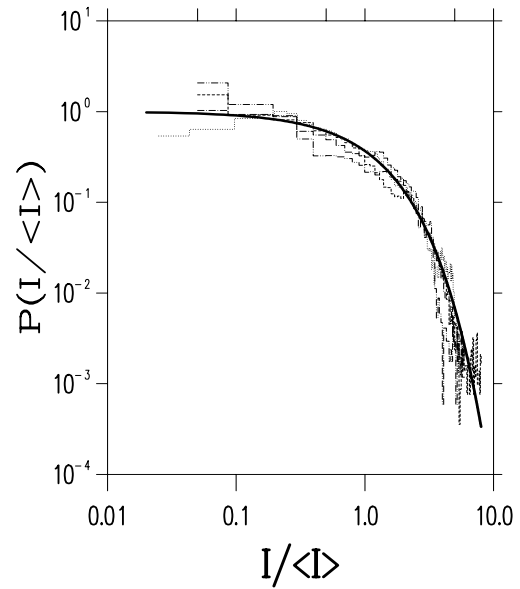


FIG. 3. Probability distribution for MS intensities in a DLEED model. Different energies are shown. (a) Thick solid line: χ_2^2 law; (b) dotted: $E = 12$ a.u.; (c) dashed: $E = 14$ a.u.; (d) dashed dotted: $E = 16$ a.u.; (e) dashed two-dotted: $E = 11.1$ a.u. (experimental).

Figure 4

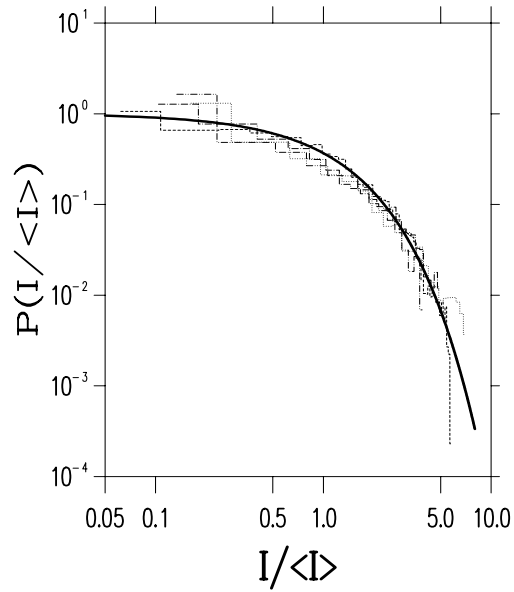


FIG. 4. Probability distribution for MS intensities in a LEED model. Different materials are shown. (a) Thick solid line: Porter-Thomas law; (b) dotted: Cu(100); (c) dashed: W(100); (d) dashed dotted: Si(111); (e) dashed two-dotted: $c(8 \times 2)\text{GaAs}(100)$ (experimental).